Materials Transactions, Vol. 46, No. 11 (2005) pp. 2419 to 2425
Special Issue on Lead-Free Soldering in Electronics III
©2005 The Japan Institute of Metals

Microstructure Control in Sn–0.7 mass%Cu Alloys

Kazuhiro Nogita[1,*], Jonathan Read[1], Tetsuro Nishimura[2], Keith Sweatman[2], Shoichi Suenaga[2] and Arne K. Dahle[1]

[1]*Materials Engineering, The University of Queensland, St. Lucia, Brisbane 4072, Australia*
[2]*Nihon Superior Co., Ltd., NS Bldg., Suita 564-0063, Japan*

Soldering alloys based on the Sn–Cu alloy system are amongst the most favourable lead-free alternatives due to a range of attractive properties. Trace additions of Ni have been found to significantly improve the soldering characteristics of these alloys (reduced bridging etc.). This paper examines the mechanisms underlying the improvement in soldering properties of Sn–0.7 mass%Cu eutectic alloys modified with concentrations of Ni ranging from 0 to 1000 ppm. The alloys were investigated by thermal analysis during solidification, as well as optical/SEM microanalyses of fully solidified samples and samples quenched during solidification. It is concluded that Ni additions dramatically alter the nucleation patterns and solidification behaviour of the Sn–Cu_6Sn_5 eutectic and that these changes are related to the superior soldering characteristics of the Ni-modified Sn–0.7 mass%Cu alloys.

(Received May 19, 2005; Accepted August 9, 2005; Published November 15, 2005)

Keywords: *lead-free soldering, nickel, eutectic, solidification*

1. Introduction

Soon after Nishimura's discovery that the presence of trace amounts of Ni in Sn–0.7 mass%Cu[1–3] alloys improves soldering properties, the Sn–Cu alloy system became one of a number of promising lead-free soldering alloys available.[4,5] The addition of between 20 and 1000 ppm Ni significantly improves the soldering characteristics of Sn–Cu alloys by reducing the tendency for "bridging" and improving the interface between the solder and the base metal.[3,6] Figure 1 shows an example of wave soldered structures on electronic circuit boards performed using Sn–0.7 mass%Cu alloys with and without trace level (600 ppm) additions of Ni. The "bridging" tendency, which can be described as the potential for webs of solder to form between adjacent terminations (resulting in a short circuit), is significantly less in the Sn–0.7 mass%Cu alloy with the Ni addition—See Fig. 1(b) compared to the equivalent Ni free alloy in Fig. 1(a).

The phase diagram of the Sn–Cu system contains a eutectic reaction at Sn–0.7 mass%Cu[7] and 227°C. This eutectic reaction is between the intermetallic Cu_6Sn_5 and Sn. In other eutectic alloy systems, modification of the eutectic microstructure by trace element addition is widely practiced. For example, in hypoeutectic Al–Si alloys[8] the eutectic silicon is modified by trace level additions of strontium or sodium and this effect has been explained by an impurity induced twinning growth mechanism.[9] In Al–Si alloys modification results in a structural transformation of the leading Si phase from a plate-like to a fine fibrous morphology. This is significant for the Sn–Cu system as Wu *et al.*[10] reported that trace concentrations of rare earth elements significantly modify both the primary phase morphology and the eutectic microstructure of Sn–0.7 mass%Cu alloys, suggesting that this alloy system is also susceptible to microstructural control by the addition of trace elements. Huh *et al.*[11,12] also reported that Ag (up to 1 mass%) and Au (up to 3 mass%) refined primary Sn and eutectic Sn–Cu microstructures, and that this refinement also lead to improved mechanical properties. However, with the exception of this research there is little known about eutectic modification in the Sn–Cu alloy system.[10–13]

The purpose of the current research is to investigate if trace level additions of Ni modify the eutectic Sn–Cu_6Sn_5 microstructure and if such modification could be responsible for the improvement in soldering properties obtained when Ni is present in Sn–Cu alloys. The alloys were investigated by thermal analysis during solidification, as well as optical/SEM microanalyses of fully solidified samples and samples quenched during solidification.

2. Experimental

Eutectic Sn–Cu alloys of nominal composition Sn–0.7 mass%Cu were used for the experiments. The chemical composition of the experimental alloys with additions of 0, 100, 600 and 1000 ppm Ni is given in Table 1. The alloys were produced in a clay-graphite crucible and heated in an electric resistance furnace to a temperature of 300°C.

Thermal analysis and quenching experiments were performed in tapered stainless-steel cups coated with a thin layer of boron nitride as shown in Fig. 2. The cooling rate just prior to nucleation of the eutectic phase was about 0.25 K/s. Two samples were taken in parallel, one with and one without a thermocouple, by submerging the stainless steel cups into the clay-graphite crucible. During solidification the cooling curve from the thermocouple was monitored on a real-time display and the sample without a thermocouple was quenched at a desired stage during solidification. Although it is acknowledged that solidification will not proceed identically in both cups, this method prevents the thermocouple from interfering with solidification or from damaging the microstructure during quenching.

Two characteristic temperatures were determined for each reaction detected on the cooling curves according to the method of Tamminen.[14] These temperatures were the

*Corresponding author, E-mail: k.nogita@minmet.uq.edu.au

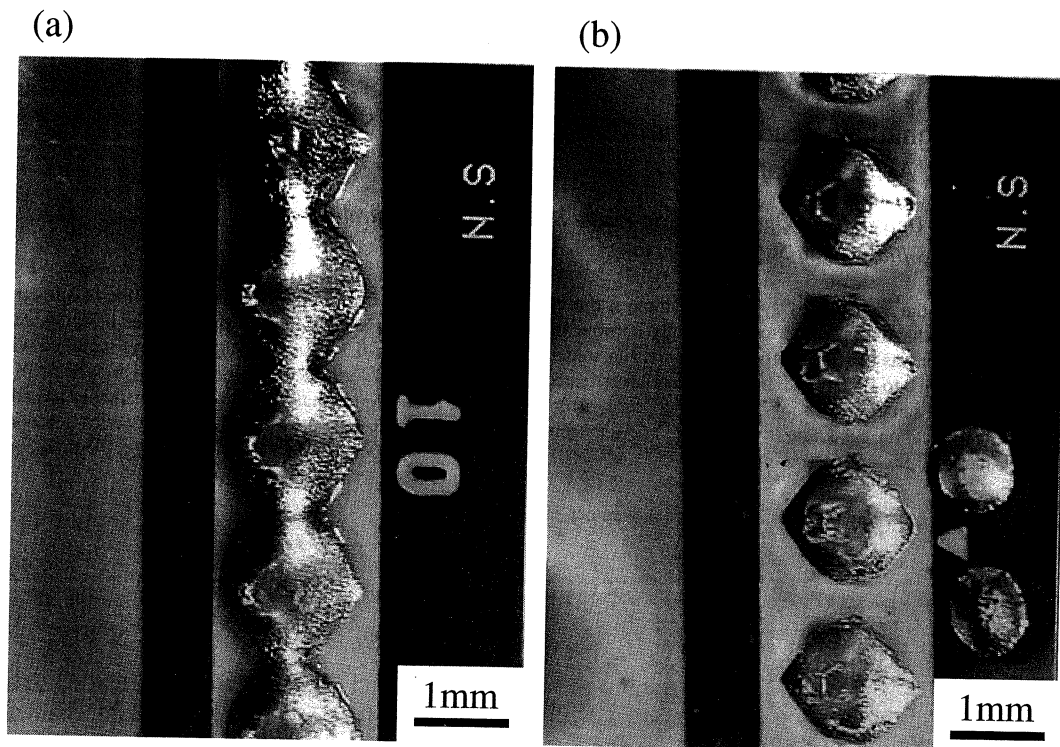

Fig. 1 Wave soldering at 250°C, 3–4 s contact time. (a) Sn–0.7 mass%Cu and (b) Sn–0.7 mass%Cu–0.06 mass%Ni. Trace level addition of Ni makes dramatic improvement of "bridging".

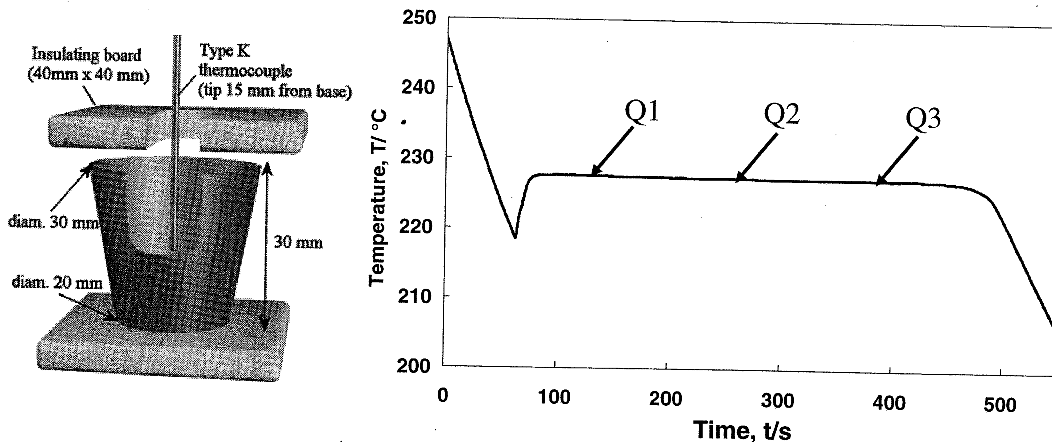

Fig. 2 A schematic (cut-away and exploded for clarity) of the experimental set-up for thermal analysis. Two samples were taken simultaneously, one with and one without a thermocouple, the cup without a thermocouple was quenched approximately half-way through solidification. An example cooling curve showing the quench location (Q1: 120 s from the point of undercooling, Q2: 220, and Q3: 320) are also shown.

Table 1 Chemical compositions of the samples (mass%).

Sample	Sn	Cu	Ni	Pb	Sb	Ag	Zn	Al	Fe
Ni-free	Bal.	0.63	0.004	0.04	0.02	<.005	<.005	<.005	0.006
100 ppm Ni	Bal.	0.63	0.012	0.04	0.02	<.005	<.005	<.005	0.011
600 ppm Ni	Bal.	0.61	0.053	0.04	0.01	<.005	<.005	<.005	0.005
1,000 ppm Ni	Bal.	0.61	0.089	0.04	0.01	<.005	<.005	<.005	0.005

nucleation temperature, T_n, defined as the first noticeable change on the derivative of the cooling curve, and the growth temperature, T_g, defined as the maximum reaction temperature reached after recalescence. Solidification of the quenching samples was interrupted at a desired time during the eutectic reaction by plunging the sample into water at room temperature. Each thermocouple was calibrated prior to experimentation using commercial purity Sn.

Samples of composition Sn–0.7 mass%Cu, with and without 600 ppm Ni, were quenched at 120, 220 and 320 s from

the point of maximum undercooling in the cooling curves as shown in Fig. 2(b). These samples were then sectioned and polished to investigate the macrostructure of the alloys. Each of the samples was sectioned, mounted in resin and then ground using SiC paper (120–2400 grit). The samples were then given a final grinding, using 4000 grit SiC paper using soap as a lubricant to prevent the embedding of abrasive particles, before a final polishing using 0.05 µm colloidal silica. Macrographs were taken of these samples before and after etching in a 5% HNO_3 solution. A JEOL 6460LA scanning electron microscope was used in low vacuum mode to take high magnification backscattered electron images (BEI) and energy dispersive spectra (EDS) of the samples with particular focus on determining the location of Ni in the microstructures.

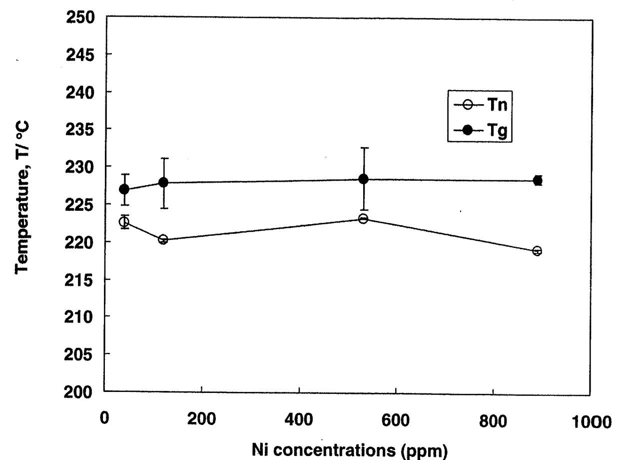

Fig. 3 Nucleation (T_n) and growth (T_g) temperature vs. Ni concentrations.

3. Results

3.1 Thermal Analysis and microstructure of fully solidified samples

Figure 3 is a plot of the eutectic nucleation (T_n) and growth temperatures (T_g) with respect to Ni concentration. Although there is some variation in the growth and nucleation temperatures, it is not possible to discern a clear effect within the levels of experimental accuracy. Figures 4(a)–(d) show optical micrographs of fully solidified (uninterrupted

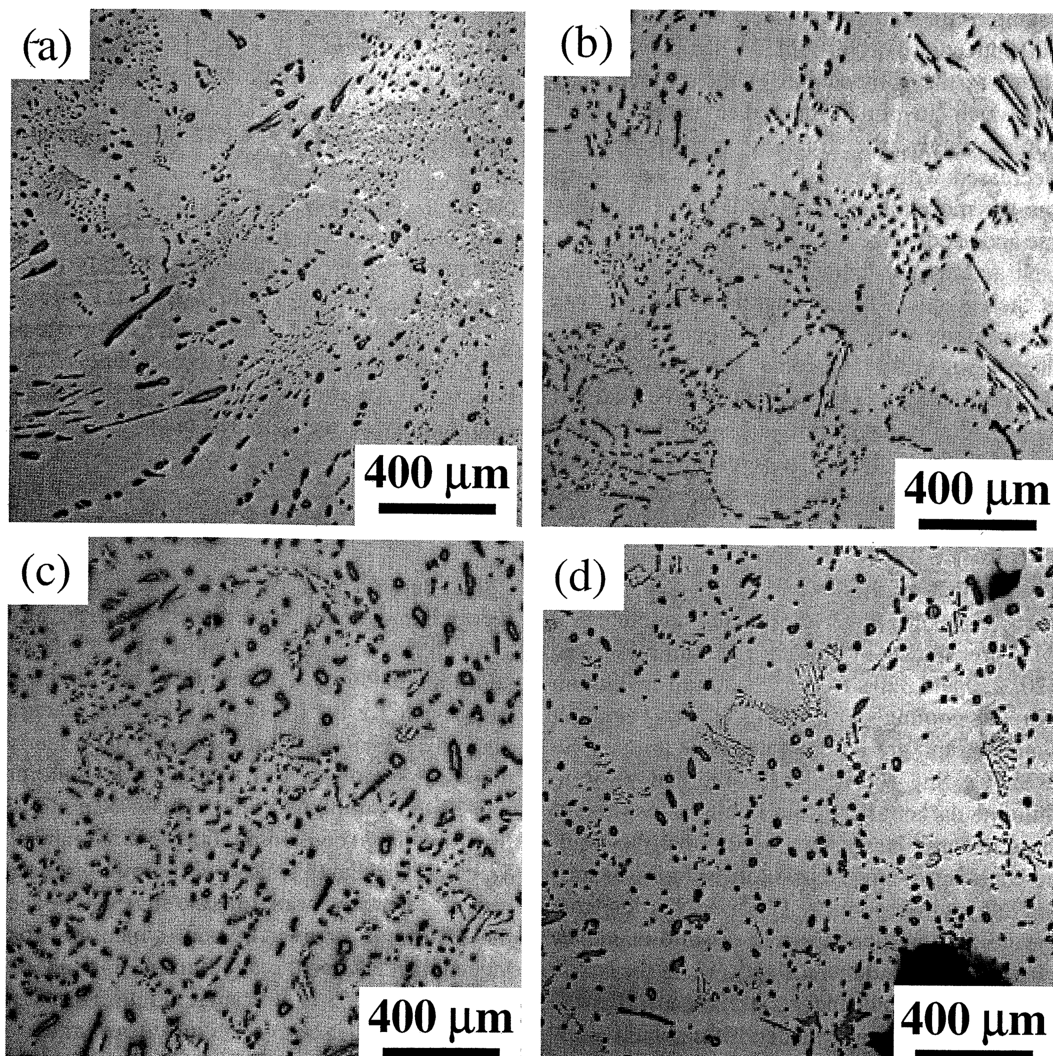

Fig. 4 Optical micrographs of fully solidified samples. (a) Sn–0.7 mass%Cu, (b) Sn–0.7 mass%Cu–100 ppm Ni, (c) Sn–0.7 mass%Cu-600 ppm Ni and (d) Sn–0.7 mass%Cu–1,000 ppm Ni.

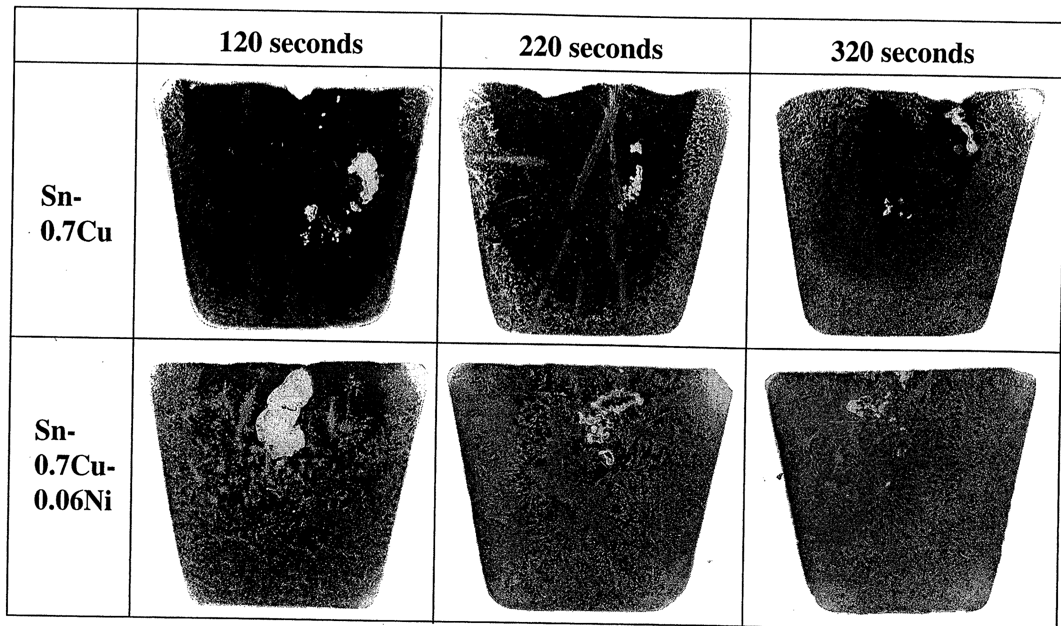

Fig. 5 Quenched microstructures during solidification. Solidification mode is changed from "Wall-type" for the 0 ppm Ni sample to "Distributed-type" in the 600 ppm Ni sample.

solidification) samples for Ni addition levels of (a) 0 ppm, (b) 100 ppm, (c) 600 ppm and (d) 1000 ppm. All samples contain some Sn dendrites as the composition of the experimental alloy is slightly rich in Sn compared to the eutectic composition. Interestingly the fraction of dendrites is significantly decreased with increasing Ni additions. With no Ni additions the morphology of the eutectic Cu_6Sn_5 is relatively coarse and needle-like. At higher Ni concentrations (*e.g.* 600 ppm Ni and above) there is a clear change in the morphology of the eutectic. This structural change involves both a slight coarsening of the eutectic accompanied by a tendency for the Cu_6Sn_5 phase to become more rounded. The regions of very refined eutectic observed without Ni addition are very few and small after the addition of Ni. Although it is difficult to conclude from these two-dimensional micrographs, it is possible that the needles are much shorter after Ni has been added.

3.2 Eutectic solidification modes

The macrostructures of quenched samples containing 0 and 600 ppm Ni are shown in Fig. 5. The samples were quenched at 120, 220 and 320 s from the point of maximum undercooling in the cooling curves [Fig. 2(b)]. The light areas in each macrograph are a combination of primary Sn dendrites and Sn–Cu_6Sn_5 eutectic that solidified prior to quenching, while the darker areas were liquid at the time of quenching. These images clearly demonstrate that the solidification front advances from the edges of the sample towards the centre in the alloy with 0 ppm Ni. The solidification front is not compact and flat, but contains a semi-solid or mushy zone with the fraction of liquid increasing towards the centre of the sample. In the samples quenched at 120 and 220 s it is seen that there are a few large Sn dendrites which grow preferentially from the base of the sample. These are believed to be dendrites which were favourably orientated for growth when the base of the cup first hit the quenching liquid. The evolution of microstructure in the alloy with an addition of 600 ppm Ni is very different (see Figs. 5 and 6), showing growth from a large number of individual nucleation sites throughout the volume of the sample with little preference for nucleation and growth from the edges of the sample. Figure 6 shows magnified optical micrographs of a sample containing 600 ppm Ni that was quenched during solidification [Fig. 6(a)] and a representative EDS/SEM analysis result taken from a fully solidified sample of the same composition [Figs. 6(b) and (c)]. Round-shaped Cu_6Sn_5 intermetallic particles are expected to be the nucleation site for eutectic Sn. EDS elemental analyses by SEM indicate that the Cu_6Sn_5 intermetallic particles contain Ni in solid solution. Detailed examination of the samples could not detect any Ni-base precipitates.

4. Discussion

The current research was conducted to determine if the reported modification of Cu–Sn eutectic alloys with rare earth elements as well as Ag and Au[10–13] also occurs with Ni additions, and if so, to determine if this modification could be responsible for the improved soldering characteristics of the alloy. The results from the quench trials clearly confirm that there are significant differences in the solidification behaviour of the unmodified Sn–0.7 mass%Cu alloy, compared to that in alloys containing 600 ppm Ni and 1000 ppm Ni. Without Ni, Sn–0.7 mass%Cu shows growth of a mushy interface that advances from the edges of the samples towards the centre; a growth mode which we call the 'wall mechanism'. After the addition of 600 and 1000 ppm Ni to this alloy, there is a change in the macroscopic growth interface, with solid evolving from a large number of nucleation centers throughout the melt. One possible reason for these differences is that nuclei have been introduced with the nickel addition and these cause a vast increase in

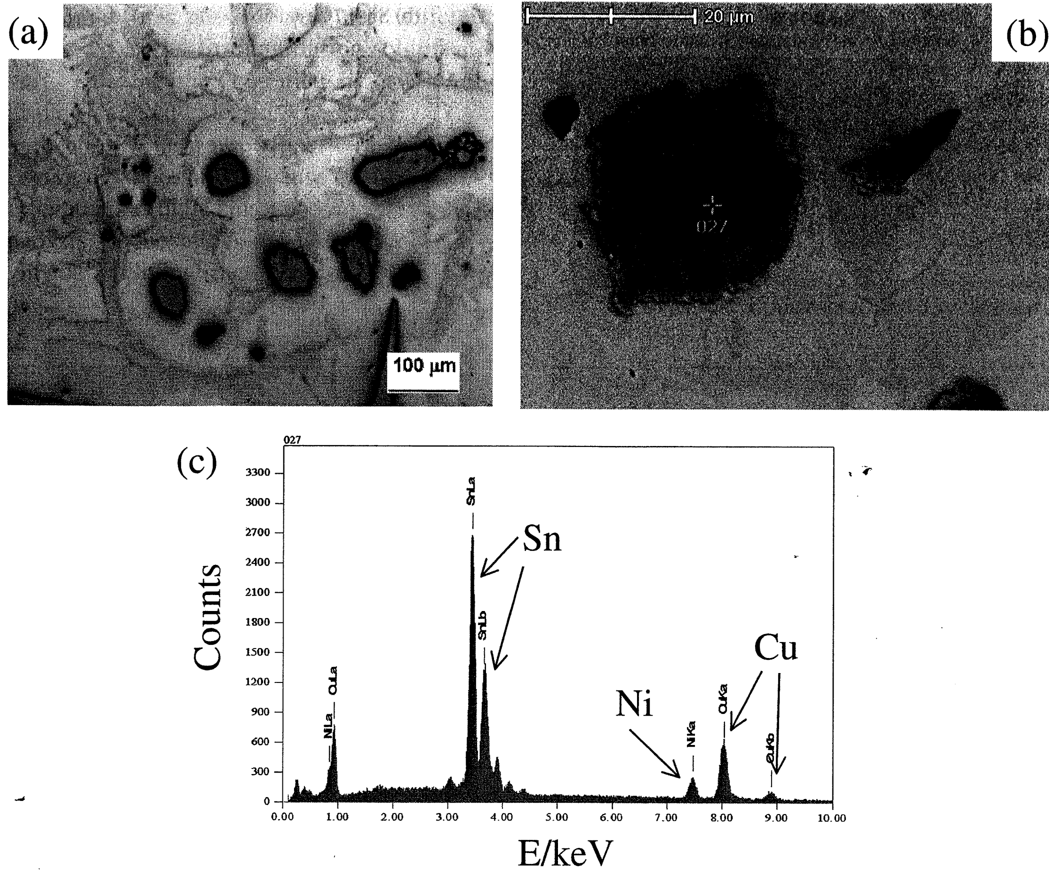

Fig. 6 (a) Quenched microstructure of 600 ppm Ni addition sample during solidification, (b) SEM image of fully solidified 600 ppm Ni addition sample, and (c) EDS analysis of eutectic Cu_6Sn_5 intermetallic particles.

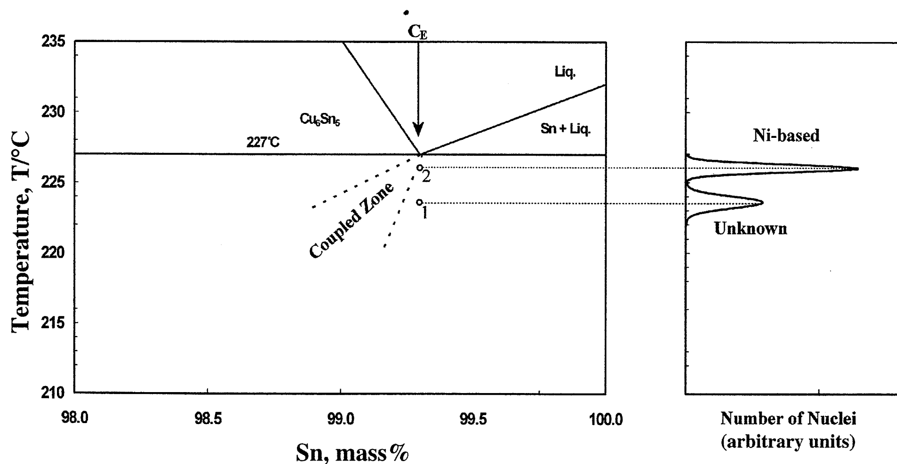

Fig. 7 An extract of the Sn-rich region of the Cu–Sn phase diagram. The point marked by 1 indicates 0 ppm Ni addition sample and marked by 2 indicates 600 ppm Ni addition sample.

nucleation potency and frequency in the alloy. A further potential explanation would be related to changes in the constitutional conditions for nucleation (*i.e.* increased constitutional undercooling). It is also possible that the solid/liquid surface tension characteristics of the alloy have changed with the addition of nickel.

The mechanism involved with an increased nucleation frequency and potency is explained with reference to Fig. 7 which shows an extract of the Sn-rich region of the Cu–Sn phase diagram (based on the phase diagram[7]). A schematic coupled zone has been added to the diagram to represent the range of compositions where coupled eutectic growth is likely to occur during non-equilibrium solidification. Due to the large difference in slopes of the liquidus lines of the two eutectic phases, the coupled zone is skewed towards the more faceted phase (Cu_6Sn_5).[15] During cooling of an alloy of eutectic composition, C_E, the temperature will decrease until nucleation and recalescence occur. With an assumption that there are relatively few nuclei of low potency in the Ni-free alloy, then undercooling will continue to a temperature

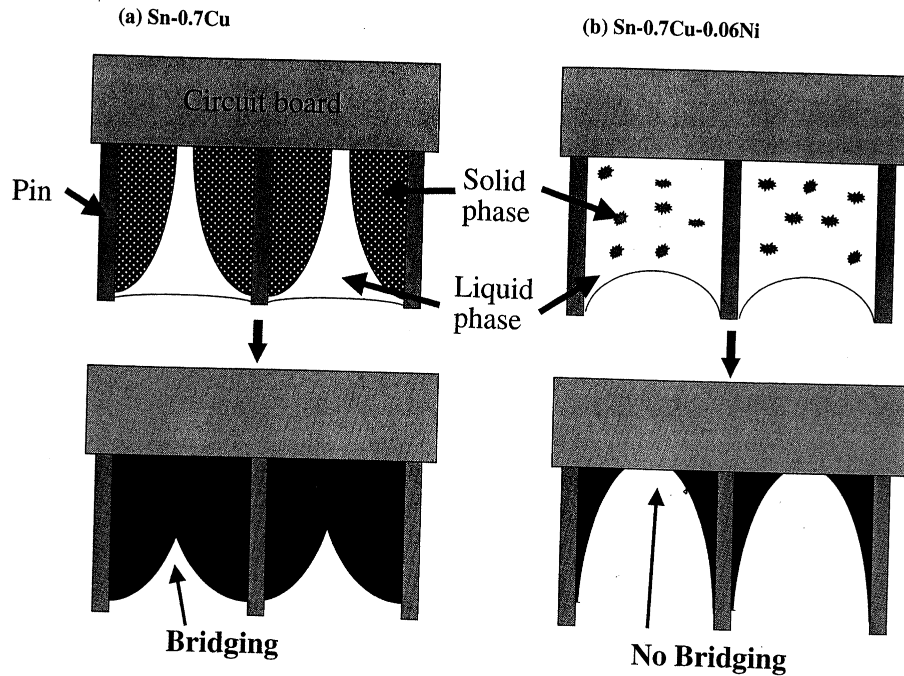

Fig. 8 A schematic illustration of the pins on a printed circuit board (PCB) and solidification of wave-solder. (a) The Sn–0.7 mass%Cu alloy freezes, growth of the solid phase occurs mainly from the walls, while (b) the solidification of the Sn–0.7 mass%Cu–0.06 mass%Ni alloy occurs from many independent growth centres present in the melt. The liquid drains more easily for the sample in (b).

marked by 1 in Fig. 7, which corresponds to the nucleation distribution marked 'unknown' but from/near "the edges" of the sample. In contrast, if the Ni addition introduces or activates a larger population of more potent nuclei, then the temperature would not drop so far and recalescence occurs at the temperature marked 2 in Fig. 7, corresponding to the distribution of nuclei marked 'Ni-based'. The skewed couple zone would lead to a relatively larger fraction of Sn dendrites in a sample that undergoes relatively more undercooling. The scenario of increased nucleation with increasing Ni additions is therefore supported by observations that additions of Ni reduce the fraction of Sn dendrites that form during solidification of Sn–0.7 mass%Cu alloys (see Fig. 4). A difference in growth temperatures is further supported by the coarser eutectic after the addition of Ni. Depending on the exact shape of the coupled zone and the relative potency of nuclei, the change in nucleation temperature between the two scenarios may have been below the resolution of cooling curve analysis, which only detects changes occurring in the bulk of the sample.

The Cu_6Sn_5 intermetallic phase has a high Ni solubility. The EDS/SEM results in Fig. 6 confirmed the presence of Ni in most Cu_6Sn_5 intermetallic particles. This may be responsible for the morphological change of the more rounded Cu_6Sn_5 intermetallics found in the alloys containing Ni. There is thus segregation of Ni occurring between the eutectic phases during solidification. The SEM analysis was unable to detect the presence of any other intermetallic phases. However, an intermetallic Ni_3Sn_2 does exist and could be expected to be very potent nuclei for the Cu_6Sn_5 intermetallic. The reason is that the very similar crystal structures and lattice spacings of Cu_6Sn_5 (hexagonal, $a = 0.4125$ nm and $c = 0.5128$ nm) and Ni_3Sn_2 (hexagonal, $a = 0.4190$ nm and $c = 0.5086$ nm), within 1.6% difference in the a-axis and 2.2% in the c-axis. However, EDS/SEM analysis failed to detect this intermetallic and further investigation of the exact nuclei for the Cu_6Sn_5 phase is required and warranted.

Regardless of the underlying causes for the different solidification behaviour of Sn–0.7 mass%Cu with and without Ni addition, they may be responsible for the improved solderability of the Sn–0.7 mass%Cu–0.06 mass%Ni alloy compared to the Sn–0.7 mass%Cu alloy. A possible scenario is schematically illustrated in Fig. 8. As the Sn–0.7 mass%Cu alloy freezes, growth of the solid phase occurs mainly from the edges of the liquid areas, which would be the pins on a printed circuit board (PCB). This leads to a narrowing region of liquid between the merging solidification fronts, and this narrow region is likely to retain liquid due to capillary forces, resulting in bridging between adjacent pins. On the other hand, solidification of the Sn–0.7 mass%Cu–0.06 mass%Ni alloy occurs from many independent growth centers present in the melt, forming an almost complete 'mushy' zone but still with a gradient in fraction solid. This latter scenario would enable any remaining mush between pins to drain away more easily (as long as a coherent network does not exist), thus possibly reducing the problem of bridging—See Fig. 8.

5. Conclusions

Samples quenched at different stages during solidification of an Sn–0.7 mass%Cu alloy shows that this alloy solidifies with a mushy interface emerging from the edges towards the thermal centre of the sample. However, Sn–0.7 mass%Cu–600 ppm Ni and Sn–0.7 mass%Cu–0.1 mass%Ni alloys display a very different solidification pattern, with a large number of independent grains growing throughout the

volume of the sample. It is possible that these differences occur due to Ni based nuclei forming during solidification, possibly Ni_3Sn_2. This idea is supported by a nucleation analysis based on a coupled eutectic zone that skews away from the Sn rich phase, but is not supported by the results from cooling curve data, possibly because any difference in nucleation temperatures is quite small and thus not resolved. EDS/SEM analysis of the alloys revealed that the Ni is concentrated in the CuSn-intermetallics, probably in solid solution.

Acknowledgements

The authors acknowledge Dr. J. Gates, UQ Materials Performance, and Dr. S. D. McDonald, the University of Queensland, for their support and stimulating discussions.

REFERENCES

1) T. Nishimura: International Patent No. EP1043112, "Lead-free solder", 28 September 1999.
2) T. Nishimura: US Patent No. US6180055, "Lead-free solder alloy", 24 November 1999.
3) T. Nishimura, S. Suenaga and M. Ikeda: The Fourth Pacific Rim International Conference on Advanced Materials and Processing (PRICM4), (eds. S. Hanada, Z. Zhong, S. W. Nam and R. N. Wright) (The Japan Institute of Metals, Honolulu, Hawaii, USA, 2001) 1087–1090.
4) T. Nishimura: Materia Japan **43** (2004) 651–654.
5) S. Suenaga, M. Yoshimura, T. Nishimura and M. Ikeda: *10th Symposium on Microjoining and Assembly Technology in Electronics*, (Yokohama, Japan, 2004) 13–16.
6) H. Nishikawa, J. Y. Piao and T. Takemoto: *2nd International Conference on Lead Free Electronics*, (Amsterdam, 2004) 1–4.
7) M. Hansen and K. Anderko: *Constitution of Binary Alloys* (McGraw Hill, 1958).
8) K. Nogita, S. D. McDonald, J. W. Zindel and A. K. Dahle: Mater. Trans. **42** (2001) 1981–1986.
9) S. Z. Lu and A. Hellawell: Metall. Trans. A **18A** (1987) 1721–1733.
10) C. M. L. Wu, D. Q. Yu, C. M. T. Law and L. Wang: J. Electron. Mater. **31** (2002) 928–932.
11) S. H. Huh, K. S. Kim and K. Suganuma: Mater. Trans. **42** (2001) 739–744.
12) S. H. Huh, K. S. Kim and K. Suganuma: Mater. Trans. **43** (2002) 239–245.
13) C. M. L. Wu, D. Q. Yu, C. M. T. Law and L. Wang: Mater. Sci. & Eng. R-Reports **44** (2004) 1–44.
14) J. Tamminen: Ph.D. Thesis, Stockholm University, 1988.
15) W. Kurz and D. J. Fisher: *Fundamentals of solidification* (Trans Tech Publications Ltd., Switzerland, 1998) pp. 110.